FEBS 17994 FEBS Letters 400 (1997) 215–220

Cloning, expression and CNS distribution of Kv4.3, an A-type K^+ channel α subunit

Meei-Ling Tsaur[a,*], Chaio-Chaio Chou[a], Yang-Hsin Shih[b], Hung-Li Wang[c]

[a]*Institute of Neuroscience, National Yang-Ming University, Taipei 112, Taiwan, ROC*
[b]*Division of Neurosurgery, Neurological Institute, Veterans General Hospital, Taipei 112, Taiwan, ROC*
[c]*Department of Physiology, Chang Gung College of Medicine and Technology, Tao-Yuan 333, Taiwan, ROC*

Received 2 October 1996

Abstract A full-length K^+ channel cDNA of Kv4.3, with an open reading frame of 611 amino acids, was isolated from rat hippocampus. Functional expression of Kv4.3 cDNA in *Xenopus* oocytes revealed an A-type K^+ channel. In the central nervous system, Kv4.3 is most prominently expressed in the retrosplenial cortex, medial habenula, anterior thalamus, hippocampus, cerebellum, as well as lateral geniculate and superior colliculus, which are important for vision. The abundant expression of Kv4.3 in many CNS neurons supports its important role as a major component of subthreshold A currents in the control of action potentials and thus neuronal excitability.

Key words: Voltage-dependent potassium channel; cDNA cloning; A-type potassium channel; *Xenopus* oocyte; In situ hybridization

1. Introduction

Voltage-dependent K^+ (Kv) channels are crucial in the control of electric signaling, which is important for the coding and processing of information in the nervous system [1,2]. Kv channels consist of α and β subunits [3]. α subunits are sufficient to form functional K^+ channels, evoking either delayed rectifier or A-type outward K^+ currents when expressed in *Xenopus* oocytes [4–6]. β subunits can modulate α subunits by accelerating the rate of inactivation [7,8]. A large family of mammalian α subunits were isolated and divided into six subfamilies (Kv1–Kv6) based on amino acid homology [9].

The Kv4 members Kv4.1, Kv4.2, and Kv4.3 have been suggested to be the major components of the subthreshold A currents (I_{SA}) detected in central neurons [10]. A-type K^+ current (I_A) is transiently activated and rapidly inactivated during depolarization in which other types of K^+ currents are not inactivated [1]. To subdivide from I_A which is activated over a wide range, I_{SA} is activated at negative membrane potentials below the threshold of Na^+ action potential [10]. I_{SA} thus controls the timing, duration, frequency, and number of action potentials [1]. In *Xenopus* oocytes, Kv4.1 or Kv4.2 was shown to conduct I_A when expressed alone [11,12], but the property of K^+ current resembled I_{SA} when co-expressed with modification factors isolated from brain [10,13]. The unidentified factors might be similar to β subunits which have been shown to modify the properties of α subunits [7,8]. With only the partial coding sequence of Kv4.3 known [14], whether Kv4.3 alone also evoked I_A in *Xenopus* oocytes was not clear.

*Corresponding author. Fax: (886) (2) 820-0259.
E-mail: mltsaur@ym.edu.tw

In this report, using Kv4.2 as probe [12,15], we isolated a full-length cDNA of Kv4.3, and demonstrated that it encodes an A-type K^+ channel α subunit when expressed in *Xenopus* oocytes. Furthermore, mapping the CNS expression pattern of the Kv4.3 gene provides an informative first step toward understanding its function in central neurons.

2. Materials and methods

2.1. cDNA cloning and sequencing

The 0.6 kb *NcoI*/*KpnI* fragment of the Kv4.2 cDNA encoding S1–S5 and part of H5 was used as probe and labeled with [α-^{32}P]dCTP, in the screening of a rat hippocampus λZAP II cDNA library as described [12]. Both strands of Kv4.3 cDNA were sequenced.

2.2. In vitro transcription/translation

In the presence of T3 RNA polymerase and [^{35}S]methionine, proteins were synthesized from plasmid pBluescript SK^- with different cDNA inserts by a coupled transcription/translation system of rabbit reticulocyte lysate (Promega, Madison, WI). Aliquots of the reaction products were separated by 7.5% SDS-PAGE. The gel was dried and the pattern was visualized by X-ray film autoradiography.

2.3. Synthesis of cRNA and functional expression in Xenopus oocytes

To synthesize capped cRNA, Kv4.3/SK^- was linearized with *HpaI* and transcribed by T3 RNA polymerase. *Xenopus* oocytes were injected with cRNA in water by a digital microdispenser (510X, Drummond, Broomall, PA). Two to four days later, whole-cell membrane currents were recorded with a two-electrode voltage clamp amplifier (Oocyte Clamp OC-725A, Warner Instruments, Hamden, CT). The external solution consisted of (in mM): NaCl, 120; KCl, 2.5; $MgCl_2$, 2; HEPES, 10, pH 7.2. Recording electrodes had a resistance of 0.5–1 MΩ when filled with 3 M KCl. Experiments were performed at room temperature (23–25°C).

2.4. Isolation of poly(A)$^+$ RNA and Northern blot

The 1.9 kb *PstI*/*KpnI* fragment of Kv4.3 cDNA encoding the 3′ non-coding region was used as probe and labeled with [α-^{32}P]dCTP. Isolation of poly(A)$^+$ RNA and Northern blot were performed as described [16].

2.5. In situ hybridization and seizure model

In the presence of [α-^{35}S]UTP, antisense and sense cRNA probes were made from plasmid SK^- containing the *PstI*/*KpnI* fragment of Kv4.3 cDNA, by T3 and T7 RNA polymerases respectively. ISH and seizure model were performed on adult rats as described [17]. Brain regions were identified according to Paxinos and Watson [18].

3. Results

3.1. Kv4.3 cDNA encodes a polypeptide with 611 amino acids

Kv4.3 cDNA was composed of 4275 bp (GenBank accession no. L48619) with an open reading frame of 611 amino acids (Fig. 1). Since a 708 bp partial cDNA corresponding to our clone 607–1311 bp with only 12 mismatches has been reported [14] and designated Kv4.3 [9], we thus also desig-

PII S0014-5793(96)01388-9

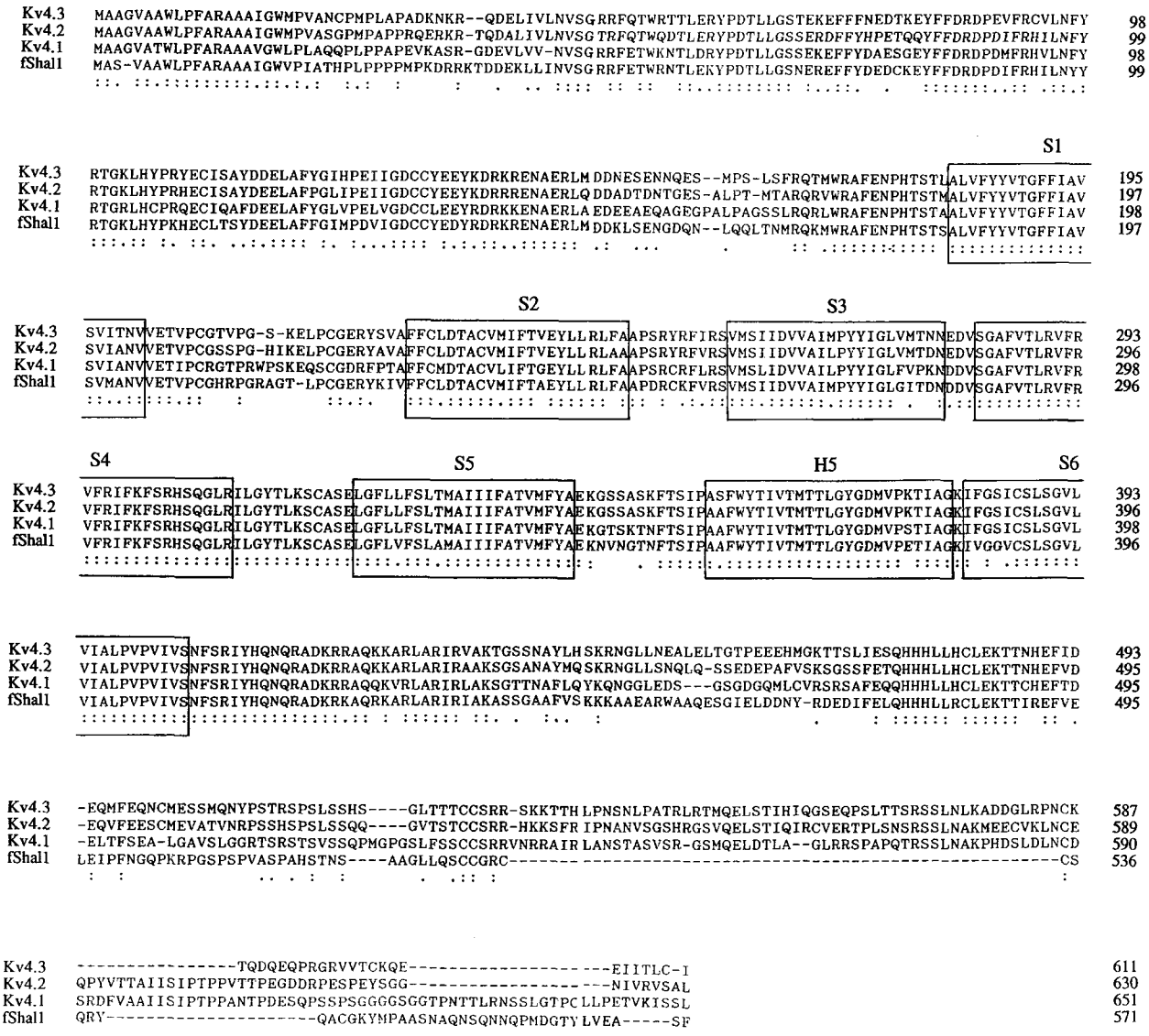

Fig. 1. Amino acid sequence alignments. The predicted amino acid sequence of rat Kv4.3 is compared with the sequences of rat Kv4.2, mouse Kv4.1 and fly Shal1 (fShal1). Dashes represent gaps. Colons represent identities. Periods represent similarities where amino acids within each of the following groups are classified as similar: A, S, and T; D and E; N and Q; R and K; I, L, M, and V; F, Y, and W [31]. S1–S6 and H5 are boxed.

nated our full-length clone Kv4.3. The deduced protein sequence of Kv4.3 contained six putative transmembrane domains S1–S6 and a pore-lining region H5, similar to other voltage-dependent K^+ channel α subunits [4–6], especially to members of the Kv4 (*Shal*-related) subfamily [9]. When aligned with rat Kv4.2 [12], mouse Kv4.1 [11] and fly Shal [19], Kv4.3 showed 76%, 67% and 64% amino acid identity, respectively (Fig. 1). When conservative amino acid substitutions were considered, there was approximately 84% similarity between the sequences of Kv4.3 and Kv4.2. Among members of the Kv4 subfamily, the protein sequences of the intracellular carboxy-terminals are most divergent; however, the functional significance of this is unknown. Furthermore, to examine whether this open reading frame encodes a polypeptide with 611 amino acids, Kv4.3 cDNA was transcribed and translated in vitro. The estimated size of 69 kDa is comparable to the predicted molecular mass value of 69 331 Da (Fig. 2).

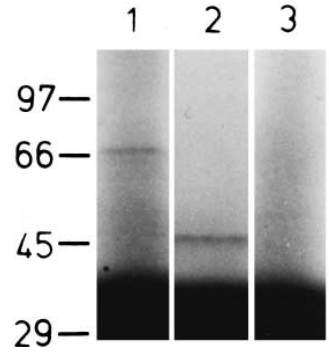

Fig. 2. Characterization of Kv4.3 polypeptide synthesized in vitro. Positions of molecular mass standards (in kDa) are shown. Lanes 1 and 2, protein products of Kv4.3 and hamster Kir3.2 [32] labeled with [^{35}S]methionine were detected at positions of 69 and 49 kDa, respectively. Lane 3, reticulocyte lysate proteins (below 35 kDa) became labeled even in the absence of exogenous mRNA.

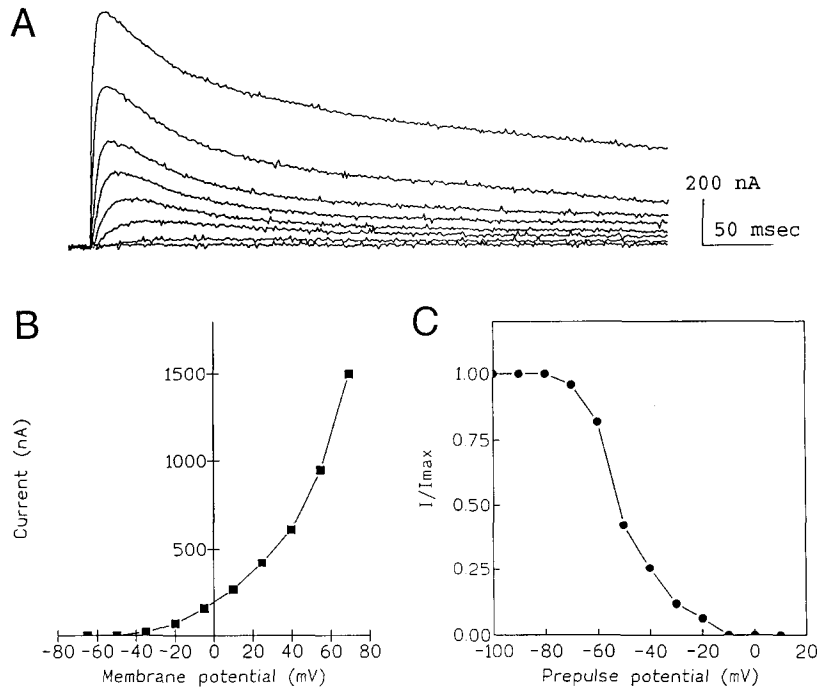

Fig. 3. Functional expression of Kv4.3 in *Xenopus* oocytes. A: Rapidly inactivating outward currents were evoked by depolarizing steps from −90 mV to holding potentials between −65 and 40 mV in 15 mV increments. The interval between voltage steps was 5 s. Leak currents were not subtracted. B: IV curves ($n=15$) were constructed by applying voltage steps from −90 mV to levels between −65 and 70 mV in 15 mV increments. One representative is shown. Note that the threshold for the activation of outward current is around −45 mV. C: One representative of a steady-state inactivation curve is shown. Oocytes ($n=7$) held at −100 mV were prepulsed for 1 s to holding potentials between −100 and 10 mV in 10 mV increments. Each prepulse was followed by a voltage step to 40 mV. The peak current following each prepulse was normalized to the maximal outward current after a prepulse to −100 mV and plotted as a function of prepulse potential.

3.2. *Kv4.3 is an A-type K^+ channel α subunit*

Injection of Kv4.3 cRNA in *Xenopus* oocytes resulted in the expression of outward currents that activated and inactivated rapidly (Fig. 3A,B). The inactivation time constant 119 ± 8 ms ($n=11$) was obtained by fitting leak subtracted outward currents (from −90 to 30 mV) with a single exponential equation. The ion selectivity was determined by measuring the reversal potential of tail currents, which were evoked by a depolarizing step from −90 to 30 mV for 30 ms followed by repolarizing steps to a membrane potential between −120 and −65 mV in 5 mV increments. With an external solution containing 2.5 mM KCl, the mean reversal potential was −94 ± 1 mV ($n=8$), a value expected for the equilibrium potential of K^+ ions. The mean holding potential for half-inactivation of Kv4.3 was −49 ± 1 mV ($n=7$, Fig. 3C). In addition, Kv4.3 K^+ currents evoked from −90 mV to 30 mV were also substantially blocked by 5 mM 4-aminopyridine (43 ± 7% block, $n=3$). These results indicate that Kv4.3 cDNA encodes an A-type K^+ channel α subunit, similar to Kv4.1 and Kv4.2 [11,12].

3.3. *Distribution of Kv4.3 mRNA in rat brain*

Using rat brain poly(A)$^+$ RNA in Northern blot analysis, we detected a unique band at 8.2 kb (Fig. 4), which was not cross-hybridized with Kv4.2 mRNA at 6.5 kb [12,15]. Using ISH, the CNS distribution pattern of Kv4.3 mRNA could be easily recognized by its strong expression in the retrosplenial cortex and superior colliculus (Fig. 5B). We also detected it in the medial habenula, hippocampal dentate granule cells (Fig. 5A), olfactory tract, anterior thalamus, substantia nigra, cerebellum (Fig. 5B), anteroventral thalamus and lateral geniculate (Fig. 5C).

At the cellular level, in the hippocampus, Kv4.3 gene was most abundantly expressed in the dentate granule cells, abundantly in the CA3 pyramidal cells, but low in the CA1 pyr-

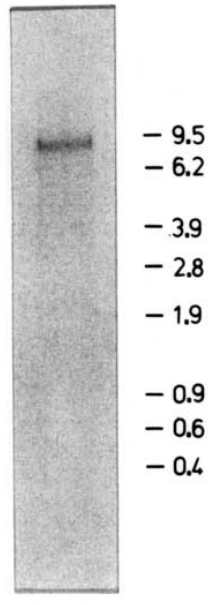

Fig. 4. Northern blot analysis of Kv4.3 mRNA. Poly(A)$^+$ RNA (14 μg) from adult rat brain was used. The positions of RNA size standards are shown.

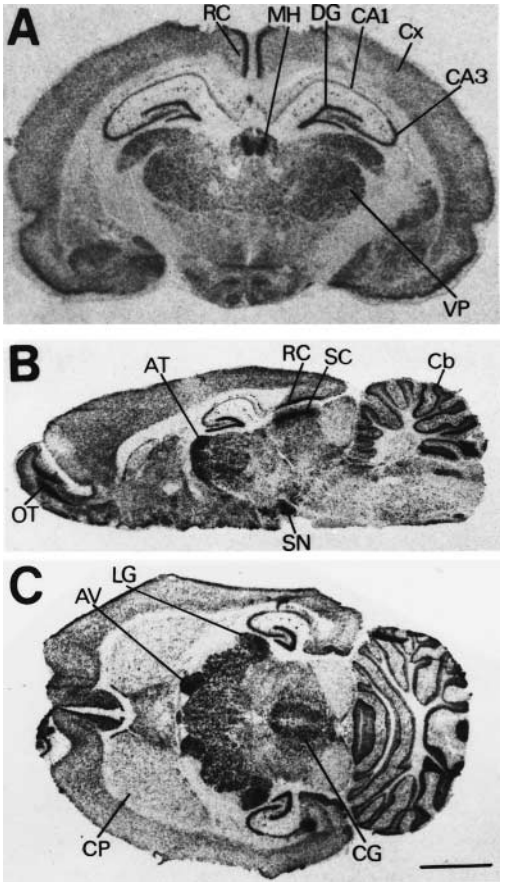

Fig. 5. CNS distribution of Kv4.3 mRNA. X-ray film autoradiograms of coronal (A), sagittal (B), and horizontal (C) sections of adult rat brain after ISH with antisense RNA probe are shown. ISH with sense RNA probe gave little signal and was used as control of background (data not shown). AT, anterior thalamus; AV, anteroventral thalamus; CA1, CA1 pyramidal cells; CA3, CA3 pyramidal cells; Cb, cerebellum; CG, central gray; CP, caudate putamen; Cx, cerebral cortex; DG, hippocampal dentate granule cells; LG, lateral geniculate; MH, medial habenula; OT, olfactory tract; RC, retrosplenial cortex; SC, superior colliculus; SN, substantia nigra; VP, ventral posterior thalamus. Scale bar: A, 2.0 mm; B and C, 3.0 mm.

amidal cells (Fig. 6A). In a previous study, we found that Kv4.2 mRNA was down-regulated in the dentate granule cells after a brief seizure activity in living animals [17]. Here, with the same treatment, we found no change of Kv4.3 mRNA in the dentate granule cells or other central neurons (data not shown). Kv4.3 was also strongly expressed in neurons scattered in the layers of stratum oriens, stratum radiatum and stratum lacunosum moleculare (Fig. 6A), as well as dentate hilus (Fig. 6B). In the cerebellum, it was found most abundantly in the Purkinje cells, and abundantly in the cerebellar nuclei, the granule cell layer, and some cells scattered in the molecular layer (Fig. 6C). In addition, Kv4.3 was highly expressed in the medial geniculate and the dorsolateral geniculate, and moderately in the ventrolateral geniculate (Fig. 6D). It was more concentrated in the lateral-lower part than the medial-upper part of the medial habenula (Fig. 6E). Furthermore, Kv4.3 mRNA was obviously detected in the pyramidal neurons of the retrosplenial cortex layer III (Fig. 6E,F), and most prominent in certain neurons scattered in the bottom area of the superficial gray layer of the superior colliculus (Fig. 6F,G). We observed distribution of Kv4.3 mRNA in many central neurons, however, the possibility that Kv4.3 is also expressed in glial cells has not been excluded.

The CNS distributions of Kv4.2 and Kv4.3 mRNAs are compared in Table 1. In summary, they are different, overlapping in some regions but complementary in others, in which Kv4.3 is more widely distributed than Kv4.2.

4. Discussion

Several other A-type K^+ channel α subunits in other subfamilies, such as Kv1.4 [20], Kv3.3 [21] and Kv3.4 [22], were also expressed in the CNS [23,24]. Nevertheless, unlike Kv4 members, they do not contribute to the I_{SA} detected in vivo

Table 1
Distribution of Kv4.3 and Kv4.2 mRNAs in the CNS

Brain region	Kv4.3	Kv4.2
Cortex		
Neocortex	+	+
Entorhinal cortex	++	+
Retrosplenial cortex	++++	++
Hippocampus		
CA1 pyramidal cells	+	++++
CA3 pyramidal cells	+++	++
Dentate granule cells	++++	+++
hilus	++	−
Stratum oriens	++	−
Stratum radiatum	++	−
Stratum lac. mol.	++	−
Subiculum	+/−	−
Amygdala	++	++
Olfactory tract	+++	+
Cerebellum		
Purkinje cells	++++	−
Granule cell layer	+++	++++
Molecular layer	+++	−
Deep nuclei	+++	−
Basal ganglia		
Caudate putamen	−	++
Globus pallidus	+	+/−
Substantia nigra	++++	+/−
Epithalamus		
Medial habenula	++++	++++
Lateral habenula	++	+
Thalamus		
Anterodorsal nu.	+++	+
Anteroventral nu.	++++	+
Anteromedial nu.	+++	+
Laterodorsal nu.	++	+
Lateroposterior nu.	++	++
Mediodorsal nu.	++	++
Ventral lateral nu.	+++	++
Ventral posterolateral nu.	+++	++
Posterior nu.	+	++
Geniculate		
Dorsolateral	++++	++
Ventrolateral	++	+
Medial	++++	++
Lower brain stem		
Central gray	+++	+
Inferior colliculus	+/−	+/−
Superior colliculus		
Superficial gray layer	++++	+
Intermediate gray layer	+	+
Deep gray layer	+	+

In situ hybridization signals were rated according to the relative grain density of Kv4.3 and Kv4.2, respectively: ++++, most abundant; +++, abundant; ++, moderate; +, low; +/−, very low but clearly above background; −, background level.

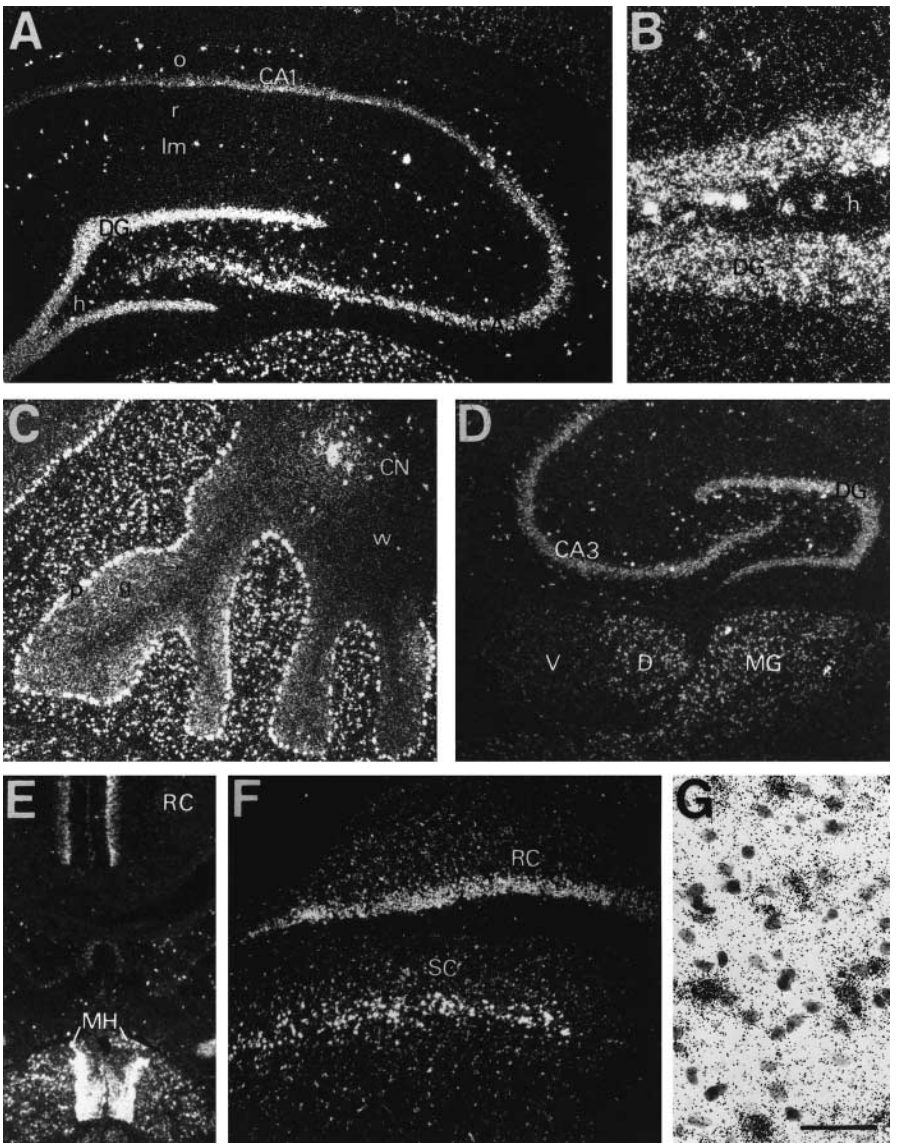

Fig. 6. Localization of Kv4.3 mRNA in selected brain regions. Dark-field (A–F) and bright-field (G) microscopic photographs of emulsion autoradiograms following ISH are shown. A: Hippocampus (coronal section). B: Higher magnification of dentate hilus (coronal section). C: Cerebellum (sagittal section). D: Geniculate bodies (horizontal section). E: Retrosplenial cortex and medial habenula (coronal section). F: Superior colliculus and retrosplenial cortex (sagittal section). G: Higher magnification of superior colliculus in area with the highest grain density (sagittal section, counterstained with toluidine blue). CN, cerebellar nuclei; D, dorsolateral geniculate; g, cerebellar granule cell layer; h, dentate hilus; lm, stratum lacunosum moleculare; m, cerebellar molecular layer; MG, medial geniculate; o, stratum oriens; p, Purkinje cell layer; r, stratum radiatum; V, ventrolateral geniculate; w, cerebellar white matter. Scale bar: A, 430 μm; B, 80 μm; C, 370 μm; D, 450 μm; E, 640 μm; F, 370 μm; G, 45 μm.

[10]. Here, consistent with the I_{SA} detected in the cerebellum and thalamus [10], we found Kv4.3 was highly expressed in these brain regions. Since the complete coding sequence of Kv4.3 was not known then, by the antisense hybrid arrest analysis, Kv4.2 was found to be the major contributor to the I_{SA} among the Kv4 members [10]. With the full-length Kv4.3 sequence available in this report, we noticed that the oligonucleotide used to arrest Kv4.2 expression had only two mismatches (2 in 22, in the 3′ end) to the corresponding Kv4.3 sequence. It is likely that I_{SA} contributed by Kv4.3 was also arrested under that condition. Whether Kv4.3 or Kv4.2 is the major component of I_{SA} in neurons of cerebellum and thalamus needs further examination. Similar determinations have been made at the neuronal level. In the rod bipolar cells of mouse eye, where Kv1.1, Kv1.2 and Kv1.3 were co-expressed, Kv1.1 was found to be the major contributor to the delayed rectifier K^+ currents detected [25].

Among Kv channels whose CNS distribution have been examined [17,23,24,26–29], Kv4.3 is distinctive with its heavy expression in regions that are important for vision, i.e. superior colliculus and lateral geniculate. The superior colliculus receives inputs from the optic tract and is involved in visual reflexes and processing of visual information. The lateral geniculate is the main terminal station of the optic tract, which projects to the calcarine cortex (area 17) and receives fibers from the same area [30]. Without overlapping with Kv4.2, it is possible that Kv4.3 is responsible for the I_{SA} in these neurons.

At the cellular level, Kv4.2 and Kv4.3 mRNAs were co-

localized in many central neurons. At the subcellular level, Kv4.2 protein was segregated in the somatodendritic surfaces of central neurons [23]. Our immunostaining data indicated that Kv4.3 protein was the same (Tsaur et al., in preparation). Although Kv4.2 and Kv4.3 are similar in structure, electrophysiological properties and likely subcellular localization, their roles do not seem redundant. In this report, in the hippocampal dentate granule cells, unlike Kv4.2 mRNA [17], we found Kv4.3 mRNA was not down-regulated by seizure activity. This indicates that Kv4.2 and Kv4.3 have different responses to neuronal activity, suggesting they play different physiological or pathophysiological roles in neurons co-expressing them. Taken together, although many K^+ channel α subunits are similar in many respects, their functions may be quite different in vivo.

Acknowledgements: We are grateful to Jen-Wen Su and Dr. Sue Lin-Chao for useful suggestions, and Drs. Samuel H.H. Chen, Fu-Chin Liu and Jenn-Tser Pan for critical discussion of the manuscript. This work was supported by Grants NSC85-2311-B-010-003-B16 (the National Scientific Council, ROC) and VGHYM-85-S4-24 (the Joint Research Program of Veterans General Hospital and National Yang-Ming University, Tsou's Foundation, Taiwan, ROC).

References

[1] Hille, B. (1992) Ionic Channels of Excitable Membranes, Sinauer, Sunderland, MA.
[2] Kandel, E.R., Schwartz, J.H. and Jessell, T.M. (1991) Principles of Neural Science, Elsevier, New York.
[3] Isom, L.L., De Jongh, K.S. and Catterall, W.A. (1994) Neuron 12, 1183–1194.
[4] Jan, L.Y. and Jan, Y.N. (1992) Annu. Rev. Physiol. 54, 537–555
[5] Pongs, O. (1992) Physiol. Rev. (Suppl.) 72, S69–88.
[6] Hoshi, T. and Zagotta, W.N. (1993) Curr. Opin. Neurobiol. 3, 283–290.
[7] Rettig, J., Heinemann, S.H., Wunder, F., Lorra, C., Parcej, D.N., Dolly, J.O. and Pongs, O. (1994) Nature 369, 289–294.
[8] Morales, M.J., Castellino, R.C., Crews, A.L., Rasmusson, R.L. and Strauss, H.C. (1995) J. Biol. Chem. 6272–6277.
[9] Gutman, G.A. and Chandy, K.G. (1993) Semin. Neurosci. 5, 101–106.
[10] Serôdio, P., Kentros, C. and Rudy, B. (1994) J. Neurophysiol. 72, 1516–1529.
[11] Pak, M.D., Baker, K., Covarrubias, M., Butler, A., Ratcliffe, A. and Salkoff, L. (1991) Proc. Natl. Acad. Sci. USA 88, 4386–4390.
[12] Baldwin, T.J., Tsaur, M.-L., Lopez, G.A., Jan, Y.N. and Jan, L.Y. (1991) Neuron 7, 471–483.
[13] Chabala, L.D., Bakry, N. and Covarrubias, M. (1993) J. Gen. Physiol. 102, 713–728.
[14] Rudy, B., Kentros, C. and Vega-Saenz de Miera, E. (1991) Mol. Cell. Neurosci. 2, 89–102.
[15] Roberds, S.L. and Tamkun, M.M. (1991) Proc. Natl. Acad. Sci. USA 88, 1798–1802.
[16] Schwarz, T.L., Tempel, B.L., Papazian, D.M., Jan, Y.N. and Jan, L.Y. (1988) Nature 331, 137–142.
[17] Tsaur, M.-L., Sheng, M., Lowenstein, D.H., Jan, Y.N. and Jan, L.Y. (1992) Neuron 8, 1055–1067.
[18] Paxinos, G. and Watson, C. (1986) The Rat Brain in Stereotaxic Coordinates, Academic Press, San Diego, CA.
[19] Wei, A., Covarrubias, M., Butler, A., Baker, K., Pak, M. and Salkoff, L. (1990) Science 248, 599–603.
[20] Stühmer, V., Ruppersberg, J.P., Schröter, K.-H., Sakmann, B., Stocker, M., Giese, K.P., Perschke, A., Baumann, A. and Pongs, O. (1989) EMBO J. 8, 3235–3244.
[21] Vega-Saenz de Miera, E., Moreno, H., Fruhling, D., Kentros, C. and Rudy, B. (1992) Proc. R. Soc. Lond. B 248, 9–18.
[22] Schröter, K.-H., Ruppersberg, J.P., Wunder, F., Rettig, J., Stocker, M. and Pongs, O. (1991) FEBS Lett. 278, 211–216.
[23] Sheng, M., Tsaur, M.-L., Jan, Y.N. and Jan, L.Y. (1992) Neuron 9, 271–284.
[24] Weiser, M., Vega-Saenz de Miera, E., Kentros, C., Moreno, H., Franzen, L., Hillman, D., Baker, H. and Rudy, B. (1994) J. Neurosci. 14, 949–972.
[25] Klumpp, D.J., Song, E.J., Ito, S., Sheng, M.H., Jan, L.Y. and Pinto, L.H. (1995) J. Neurosci. 15, 5004–5013.
[26] Drewe, J.A., Verma, S., Frech, G. and Joho, R.H. (1992) J. Neurosci. 12, 538–548.
[27] Hwang, P.M., Glatt, C.E., Bredt, D.S., Yellen, G. and Snyder, S.H. (1992) Neuron 8, 473–481.
[28] Perney, T.M., Marshall, J., Martin, K.A., Hockfield, S. and Kaczmarek, L.K. (1992) J. Neurophysiol. 68, 756–766.
[29] Rudy, B., Kentros, C., Weiser, M., Fruhling, D., Serôdio, P., Vega-Saenz de Miera, E., Ellisman, M.H., Pollock, J.A. and Baker, H. (1992) Proc. Natl. Acad. Sci. USA. 89, 4603–4607.
[30] Parent, A. (1996) Carpenter's Human Neuroanatomy, Williams and Wilkins, Baltimore, PA.
[31] Myers, E.W. and Miller, W. (1988) Computer Appl. Biosci. 4, 35–40.
[32] Tsaur, M.-L., Menzel, S., Lai, F.P., Espinosa, R., Concannon, P., Spielman, R.S., Hanis, C.L., Cox, N.J., Beau, M.M., German, M.S., Jan, L.Y., Bell, G.I. and Stoffel, M. (1995) Diabetes 44, 592- 596.